DESIGN OF WHEAT CLEANING LOSS DETECTION DEVICE BASED ON EDEM
/
基于 EDEM 的小麦清选损失检测装置设计

Xinran SHANG*, Zehe LIU*, Hengbin ZHANG, Zushuai LI, Yujing HE*, Wanzhang WANG*
College of Mechanical & Electrical Engineering, Henan Agricultural University, Zhengzhou 450002, China;
*Corresponding authors. Tel:0371-63558040 Email: heyujinghn@henau.edu.cn; wangwz@henau.edu.cn;
[+] These authors contributed equally to this work and should be considered co-first author
DOI: https://doi.org/10.35633/inmateh-78-111

Keywords: Cleaning loss; EDEM; Wheat; ESP32; Piezoelectric ceramic sensor; Kalman filter.

ABSTRACT
Addressing the issue of high cleaning loss rates encountered during actual combine harvester operations, this study designed a detection device specifically for monitoring cleaning losses. Initially, a three-dimensional model of wheat grains was established using Blender software. Subsequently, the impact processes of wheat grains and straw falling from different heights onto a sensitive plate were simulated using EDEM discrete element analysis software, from which contact force variation curves and motion trajectories were obtained. The results indicated a significant difference in the impact forces of the two material types on the sensitive plate, enabling material identification and loss rate calculation through signal acquisition. Based on these findings, a detection device comprising a mechanical structure and a control system was developed. An ESP32 microcontroller was employed to read data from piezoelectric ceramic vibration sensors. After processing the data with a Kalman filter, material classification thresholds were determined based on the principles of normal distribution. Preliminary experimental parameters were established through a three-factor, three-level experiment, and subsequently optimized using response surface methodology. The experimental results demonstrated that optimal threshold differentiation and the highest accuracy in loss rate calculation were achieved under the following conditions: a sensitive plate installation height of 550 mm, an inclination angle of 40°, and a conveyor belt speed of 8 m/min. Bench tests verified that the overall error of the device was less than 3%, with recognition rates exceeding 97% for both wheat grains and straw.

摘要
针对实际作业中清选损失率偏高的问题，本研究设计了一种用于清选损失检测的装置。先利用 Blender 软件建立小麦籽粒的三维模型，再通过 EDEM 离散元分析软件模拟不同高度下落的小麦籽粒与秸秆对敏感板的撞击过程，获取接触力变化曲线和运动轨迹。结果显示，两类物料撞击敏感板的力度差异显著，可通过信号采集实现物料识别并计算损失率。在此基础上，设计了包含机械结构和控制系统的检测装置，采用 ESP32 单片机读取压电陶瓷振动传感器数据，经卡尔曼滤波处理后，结合正态分布规律确定物料分类阈值。通过三因素三水平实验初步确定实验参数并通过响应曲面确定实验参数，实验结果表明，当敏感板的安装高度为 550mm、倾斜角度为 40°、传送带速度 8 米/分钟时，阈值区分度最佳，损失率计算精度最高。台架实验验证表明，该装置整体误差小于 3%，对小麦籽粒和秸秆的识别率均达 97%以上。

INTRODUCTION
Loss rate serves as a critical indicator for evaluating the performance of the cleaning device in wheat combine harvesters. As a core component, the cleaning device's performance directly determines the overall cleaning effectiveness of the machine *(Zhao et al., 2023; Liu et al., 2020; Wei et al 2023; Qu et al., 2024)*. The cleaning system of a combine harvester constitutes an integral part of the machinery, and the adjustability of its operational parameters directly influences both the grain loss rate and the cleaning rate during harvesting *(Wang at al., 2018; Du et al., 2022; Yang et al., 2025)*.

Currently, the level of intelligence in combine harvester cleaning systems is generally low, with operational parameters often adjusted based on manual experience. This practice results in relatively high cleaning losses, particularly in operating environments where the feed rate varies frequently *(Ding et al., 2023; Guo et al., 2026)*. With advancements in materials science and signal processing technologies, researchers have successively developed detection sensors using sensitive materials such as piezoelectric ceramics and PVDF piezoelectric films. These sensors enable loss monitoring by collecting impact signals from grains and impurities *(Du et al., 2022; Liu et al., 2023; Chen et al., 2025; Ni et al., 2015)*.

For instance, Liu Yangchun et al. designed acorn grain loss monitoring system for a direct-cut maize grain harvester based on the piezoelectric effect. By optimizing the sensor structure and the signal processing circuit, simultaneous monitoring of cleaning losses and losses was achieved *(Liu et al., 2023; Hou et al., 2020)*. Furthermore, collision simulation analysis based on the discrete element method has provided theoretical support for optimizing sensor structures *(Ding et al., 2023)*. In the field of signal processing, traditional methods have largely relied on time-domain feature thresholds for grain identification, which presents challenges such as difficulty in threshold setting and poor robustness. To address these issues, *Xing Gaoyong et al.* proposed a signal classification method based on the VS-1D CNN model. Using impact signals collected by PVDF piezoelectric film sensors, accurate differentiation between maize grains and residues was realized, achieving a model accuracy of 94.2% *(Xing et al., 2025)*. Some recent studies have begun to incorporate modern filtering algorithms and deep learning models to enhance the accuracy and adaptability of signal classification *(Guo et al., 2026; Xing et al., 2025)*. *Ma at al., 2025,* validated the reliability of particle collision mechanics analysis using EDEM simulation, thereby providing theoretical support for establishing the identification threshold between wheat grains and straw through EDEM simulation in this study. Wei Dexin et al. designed a filter circuit based on the high-frequency differences between grain and material other than grain signals using a piezoelectric ceramic sensor, achieving the identification of corn kernels *(Wei et al 2023).*

In summary, although the progress achieved in grain loss monitoring in the field of grain loss monitoring both domestically and internationally, the devices specifically designed for loss monitoring in the wheat cleaning process remain insufficiently developed. In this study, the dynamic process of wheat grains and straw impacting a sensitive detection plate was numerically simulated using EDEM discrete element simulation software *(Peng et al., 2025; Zhang et al., 2023; Zhang et al., 2022; Ma at al., 2025; Shen et al., 2023; Liu et al., 2022; Hao et al., 2025; Li et al., 2024)*. This simulation aimed to investigate the technical feasibility of achieving precise identification of wheat grains and straw based on impact excitation signals. Leveraging the direct piezoelectric effect of piezoelectric ceramics, the electrical signals generated by impacts on the sensitive detection plate were collected in real time. These signals were transmitted via an ESP32 microcontroller to a host computer terminal. The PLX-DAQ tool *(Walkowiak et al., 2016)* was utilized for the visualization of monitoring data and for recording relevant data. Ultimately, real-time quantitative calculation of the wheat cleaning loss rate was achieved.

MATERIALS AND METHODS

Mechanical Analysis of Material Impact on the Sensing Plate

The collision between wheat grains/straw and the sensitive plate constitutes a transient impact process, and its mechanical characteristics determine the features of the sensor output signal. This process can be simplified as a mass-spring-damper system, with its dynamic equation expressed as Equation (1):

$$m\frac{d^2y}{dt^2} + c\frac{dy}{dx} + ky = F(t) \quad (1)$$

m is the Quantity, [kg];

C – Damping coefficient, [Ns/m];

k – Equivalent stiffness coefficient of the sensitive plate, [N/m];

y – Vibration displacement of the sensitive plate, [m];

$F(t)$ – Collision impact force, [N].

The impact force pulse generated by the collision can be simplified as a triangular waveform. The peak force (F_{max}) and the pulse rise time (t_r) are key characteristic parameters that determine the response signal of the sensor. According to the law of conservation of energy (Equation (2)) and Hooke's law (Equation (4), it can be deduced that the maximum impact force is related to the velocity of the material impacting the sensitive plate, the mass of the material, and the equivalent stiffness coefficient of the sensitive plate, as shown in Equation (6).

According to the law of conservation of energy:

$$\frac{1}{2}\mathrm{m}V_0^2 = \frac{1}{2}kX_{\max}^2 \quad (2)$$

can be derived:

$$X_{max} = V_0\sqrt{\frac{m}{k}} \tag{3}$$

According to Hooke's Law:

$$F_{max} = kX_{max} \tag{4}$$

Substitute into Hooke's Law:

$$F_{max} = kV_0\sqrt{\frac{m}{k}} = V_0\sqrt{mk} \tag{5}$$

$$F_{max} \propto \sqrt{V_0^2 mk} \tag{6}$$

V_0 is the velocity of material upon collision with the sensitive plate, [m/s];

m – Quality, [kg];

k – Equivalent stiffness coefficient of sensitive plates, [N/m];

F_{max} – Peak impact force, [N].

Since the duration of the force acting during the impact between the material and the sensitive plate is very short, the deformation process of the sensitive plate during its impact with the material can be simplified as a simple harmonic motion. According to the simple harmonic motion formula, it can be deduced that the rise time from the moment the sensitive plate receives the impact to the moment the impact force reaches its maximum is related to the mass of the material and the equivalent stiffness coefficient of the sensitive plate, as shown in Equation (10).

Frequency of Simple Harmonic Motion:

$$\omega = \sqrt{\frac{k}{m}} \tag{7}$$

Period of Simple Harmonic Motion:

$$T = \frac{2\pi}{\omega} = 2\pi\sqrt{\frac{m}{k}} \tag{8}$$

Time at which the collision impact force reaches its maximum:

$$t_r = \frac{T}{4} \tag{9}$$

$$t_r \propto \sqrt{\frac{m}{k}} \tag{10}$$

m is the Quantity, [kg];

k – Equivalent stiffness coefficient of sensitive plates, [N/m];

t_r – Rise time at peak collision impact force, [s].

By analyzing Equations (6) and (10), it can be deduced that the impact velocity V_0 of the material and the material mass affect both the impact force and the force rise time during the collision with the sensitive plate, resulting in differences in the contact time and impact magnitude when the material strikes the steel plate. Equation (6) indicates that the peak impact force is proportional to the material mass and velocity; the greater the mass and velocity, the larger the impact force. Equation (10) shows that the time required for the impact force to reach its maximum is proportional to the material mass. Therefore, the key to distinguishing wheat grains from straw lies in differentiating the peak force and the pulse rise time. Simulations of wheat grain and straw impacting the sensitive plate were conducted using EDEM discrete element software to measure the mechanical characteristics during impact, thereby verifying the feasibility of using the peak force and pulse rise time to differentiate between wheat grains and straw.

Establishment of the EDEM Simulation Model

Wheat grains are irregular ellipsoidal particles. By randomly selecting 100 wheat grains and measuring their length and width using a vernier caliper, the average length was determined to be l=6.31 mm, the average width w=3.24 mm, and the average thickness 2.75 mm.

The length of crushed straw after harvest by a wheat combine harvester generally ranges from 50 to 150 mm. Wheat straw segments of 50 mm and 100 mm in length were selected as experimental objects. Model construction for wheat grains was performed using Blender software. The established models were imported into EDEM discrete element simulation software. Wheat grains were filled with spherical particles of varying sizes to obtain the simulation model, while wheat straw was filled with spherical particles of identical size to construct the experimental simulation model, as shown in Figure 1. The simulation experimental parameters required for the discrete element simulation model were obtained from the literature *(Wang et al., 2020; Ma et al., 2025; Sun et al., 2021)*, as presented in Table 1.

Table 1

Parameters of EDEM Discrete Element Simulation Experiment

Simulation Parameters	Poisson's ratio	Density/(kg/m³)	Modulus of elasticity/MPa
Wheat	0.3	1480	1930
50 mm straw	0.4	1670	16.96
100 mm straw	0.4	1670	16.96
Sensing plate	0.35	1150	3000

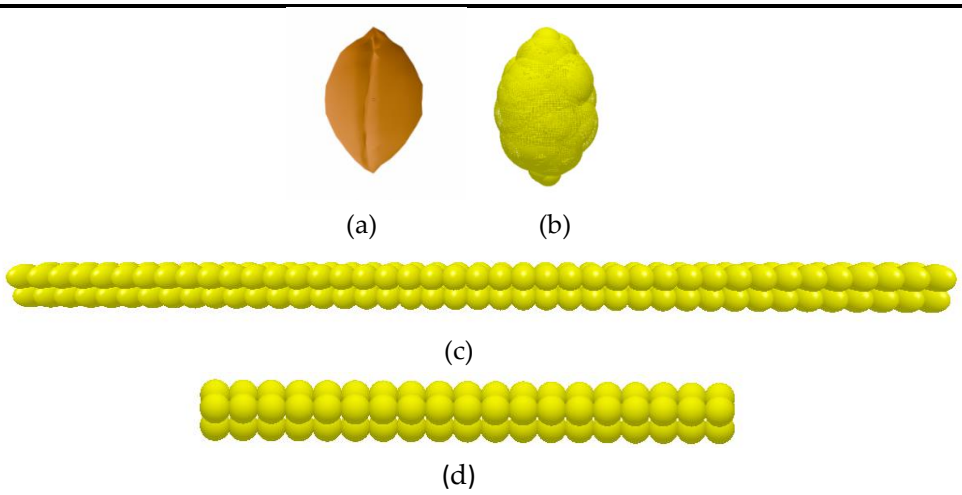

Fig. 1 - Simulation Model of Wheat and Straw

(a) Blender Wheat Grain Model; (b) EDEM wheat simulation model; (c) 100 mm Wheat Straw Model; (d) 50 mm Wheat Straw Model.

Simulation Experiment

An experimental model was established in the EDEM simulation software. Models of the conveyor belt, sensitive plate, and collection box were created according to the actual experimental dimensions, and wheat grains were generated above the conveyor belt. The distance between the conveyor belt and the center of the sensitive plate was set to 550 mm, with the sensitive plate positioned at an inclination of 40° and a conveyor belt speed of 8 m/min. Upon completion of the simulation, the material motion trajectory during a single collision event, as well as the impact force and rise time generated when the material struck the sensitive plate, were exported from the Analyst module, as shown in Figures 2 and 3.

Based on the wheat motion trajectory, it was observed that each wheat grain collided with the sensitive plate only once before falling into the collection box. This indicates that a single piece of material does not impact the sensitive plate a second time, thereby exerting no influence on the calculation of the loss rate.

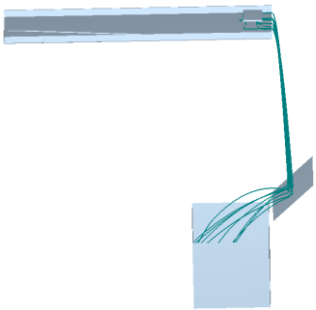

Fig. 2 - Simulation Motion Trajectory of Wheat

Based on the exported data, the duration of the impact force increase for a wheat grain colliding with the sensitive plate was 0.025 s, with a peak impact force of 0.00059 N. For a 50 mm straw segment, the duration of the impact force increase was 0.05 s, with a peak impact force of 0.0000723 N. For a 100 mm straw segment, the duration of the impact force increase was 0.09 s, with a peak impact force of 0.000153 N. As the mass of a wheat grain is less than that of straw, the rise time to reach the maximum impact force is shorter for wheat grains compared to straw. Due to the small volume and high density of wheat grains, they are less affected by air resistance during descent. In contrast, straw, characterized by its large volume, low density, and hollow structure, is significantly influenced by air resistance. Consequently, the impact velocity of wheat grains striking the sensitive plate is considerably higher than that of straw.

The experiments measured the rise time of the impact force for a wheat grain colliding with the sensitive plate as 0.025 s, with a peak impact force reaching 5.9×10^{-4} N. For a 50 mm length straw segment, the rise time was 0.05 s, with a peak impact force of 7.23×10^{-5} N. For a 100 mm length straw segment, the rise time extended to 0.09 s, with a peak impact force of 1.53×10^{-4} N. Compared to straw, wheat grains possess the physical characteristics of lower mass, smaller volume, and higher density, while straw exhibits a larger volume, lower density, and hollow structure. During the descent of both materials, the obstructive effect of air resistance on straw is significantly greater than that on wheat grains, resulting in a much higher impact velocity for wheat grains against the sensitive plate. The product of the square of the impact velocity and the mass for wheat grains exceeds that for straw; therefore, the peak impact force generated by wheat grains colliding with the sensitive plate is greater than that generated by straw. Thus, collisions involving wheat grains produce a larger F_{max} and a shorter t_r, whereas collisions involving straw produce a smaller F_{max} and a longer t_r.

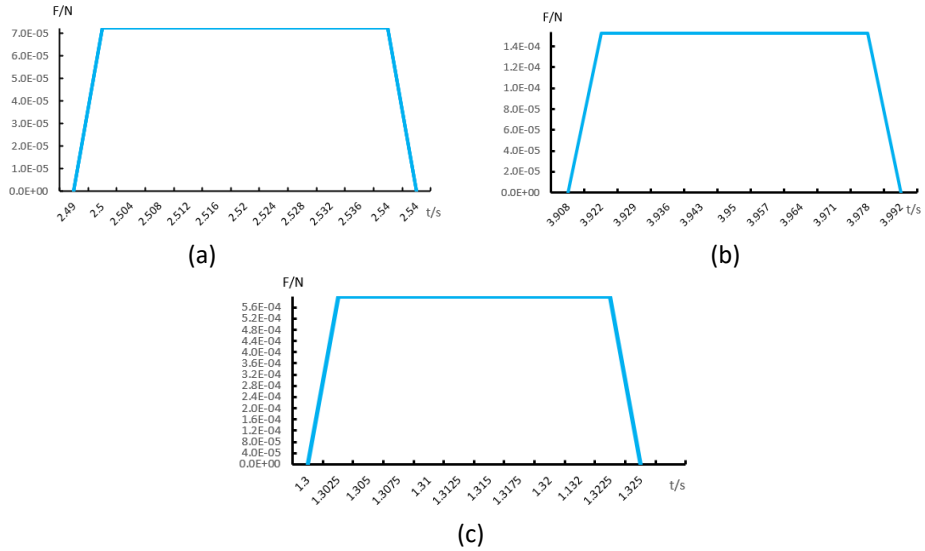

Fig. 3 - Contact Forces Between the Sensitive Plate and Wheat Grains, 50-mm Straw, and 100-mm Straw

(a) Wheat Contact Force with Sensitive Board; (b) Contact force between 50 mm straw and sensitive plate; (c) Contact force between 100 mm straw and sensitive plate.

Design of a Lower-Level Control and Processing System Based on ESP32

The analog signal pin of the piezoelectric ceramic sensor was connected to GPIO27 of the ESP32 microcontroller. This pin belongs to the ADC2 peripheral and supports high-impedance analog signal input, enabling accurate acquisition of voltage variations generated by the sensor. These analog signals were converted to digital values via the internal 12-bit ADC. To suppress ambient noise and inherent sensor noise, thereby improving the signal-to-noise ratio, a software-based Kalman filter was employed. The sensor signal was modeled as a slowly varying physical quantity over time, with its state-space representation configured as a first-order linear system. The process noise covariance was set to 0.01, and the measurement noise covariance was set to 0.2. This filter performed optimal estimation of each raw acquired value through prediction and update steps, outputting smoothed values that provided a stable and reliable data foundation for subsequent decision-making. A sliding window buffer algorithm was implemented, maintaining a buffer containing the six most recent non-zero sampled values. This algorithm aimed to capture characteristic signals appearing within a short time window and facilitate subsequent signal processing. Additionally, two function buttons were configured: one button for resetting, which clears all data and resets counters, and another button for controlling data logging. The system process is illustrated in Figure 4.

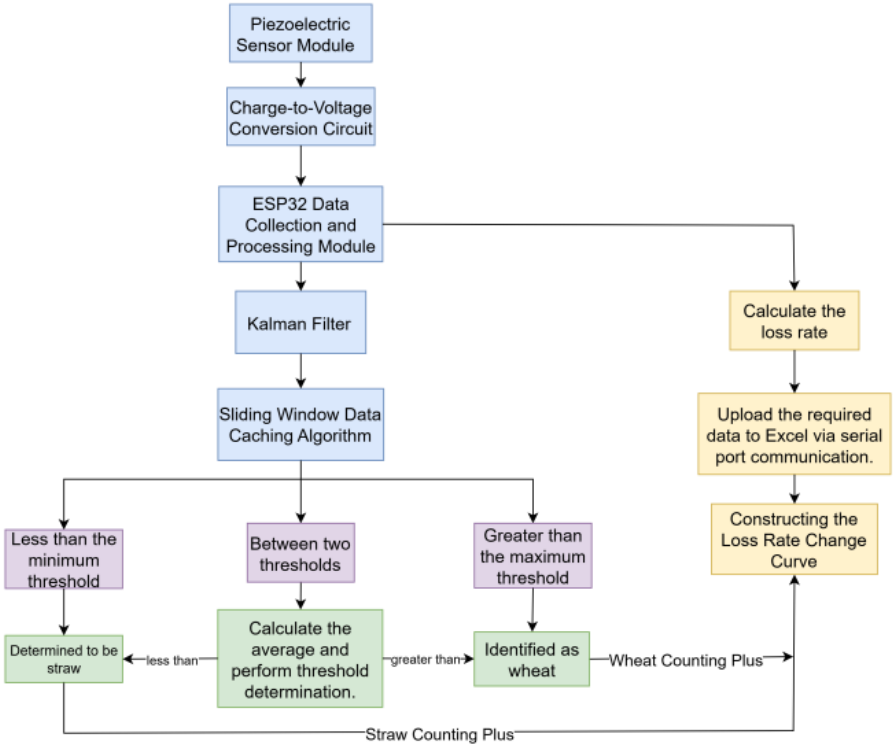

Fig. 4 - Flowchart of the Cleaning Loss Detection System

Mechanical Structure Design

The mechanical structure of the wheat loss detection device is shown in Figure 5. It is composed of a material supply box, a conveyor belt, a sensitive plate, and a collection box. Inside the material supply box, a flow-guiding and material control mechanism is designed. Under the combined action of gravity and this mechanism, wheat grains can fall from the outlet into the transport unit in a single-grain continuous state, thereby preventing interference with the detection signal caused by multiple grains falling simultaneously. The conveyor belt is responsible for transporting the material sample to be tested at a constant speed to its terminal free-fall point. Under the action of gravity, the material falls along a parabolic trajectory and impacts the central area of the inclined sensitive plate located directly below. As the core detection component, the panel of the impact-sensitive unit is positioned at a specific angle relative to the horizontal plane to ensure that wheat grains bounce and generate a distinct impact signal. After impact, the material detaches from the surface of the sensitive plate under rebound action and enters the collection box, which is used to collect the fallen material.

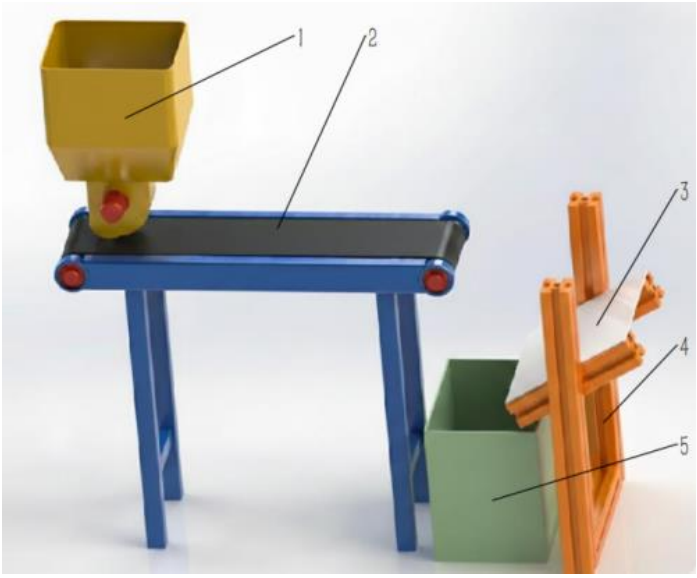

Fig. 5 - Schematic Diagram of the Overall Mechanical Structure of the Loss Detection Device

1.Feeding Device; 2.Conveyor Belt; 3.Sensitive Plate; 4.Sensitive Plate Fixing Bracket; 5.Collection Box

Orthogonal experiments determine experimental factors

To accurately achieve automatic identification and sorting of wheat grains and straw, this study determined the voltage signal threshold ranges for their impact on the sensitive plate through bench experiments. The experimental system was primarily composed of a feeding system, a conveyor belt, a sensitive plate, a data acquisition computer, and an ESP32 microcontroller-based control system. Wheat grains and wheat straw segments ranging from 50 mm to 150 mm in length were selected as experimental objects, with independent experiments conducted for each material type. For each experiment, 1000 wheat grains and 400 straw segments were randomly selected from the material stock as experimental samples.

Three key factors were considered in the experiments: the vertical installation height from the conveyor belt plane to the center of the sensitive plate, the inclination angle of the sensitive plate, and the conveyor belt speed. A three-factor, three-level orthogonal experimental design was adopted. The experimental scheme is presented in Table 2, and the orthogonal experimental tables are shown in Tables 3 and 4.

During the experiments, the system automatically completed the entire process of material conveyance, free-fall dropping, impact on the sensitive plate, and data acquisition. The dynamic response signal generated by each impact was converted from analog to digital by the ESP32 microcontroller, and the characteristic voltage values were recorded in real time using the PLX-DAQ tool. All data for different material types were imported into Origin statistical analysis software to plot their normal distribution fitting curves. The mathematical expectation (μ) of the normal distribution curve was recorded as the effective sensor data in the orthogonal experimental tables. The normal distribution plots for the orthogonal experimental data for wheat and straw are shown in Figures 6, respectively.

Range analysis was employed to process the orthogonal experiment results. For each factor, the average value of the experimental results under different levels was calculated, and the range for that factor was subsequently determined based on these averages. The magnitude of the range reflects the degree of influence of each factor on the ADC value; a larger range value indicates a more significant effect of that factor on the results.

Table 2

Experimental Factors and Levels

Level Factor	Factor		
	Installation height (mm)	Installation angle (°)	Conveyor belt speed (m/min)
1	350	30	2.7
2	450	40	5.3
3	550	45	8

Table 3

Orthogonal Experimental Design for Wheat Tests

	Orthogonal Design Table			Mathematical Expectation of Sensor Data
Number	Factor 1	Factor 2	Factor 3	
1	1	1	1	396.992
2	2	2	1	756.812
3	3	3	1	542.694
4	3	2	2	720.723
5	2	1	2	613.182
6	1	3	2	351.294
7	1	2	3	543.316
8	2	3	3	423.106
9	3	1	3	835.173
Mean 1	430.534	615.116	565.499	
Mean 2	597.700	673.617	561.733	
Mean 3	699.530	439.031	600.532	
Extreme difference	268.996	234.586	38.799	

Table 4

Orthogonal Experimental Design for Straw Tests

Number	Orthogonal Design Table Factor 1	Factor 2	Factor 3	Mathematical Expectation of Sensor Data
1	1	1	1	88.004
2	2	2	1	96.902
3	3	3	1	88.102
4	3	2	2	132.078
5	2	1	2	113.886
6	1	3	2	64.520
7	1	2	3	70.846
8	2	3	3	89.442
9	3	1	3	130.436
Mean 1	74.457	110.775	91.003	
Mean 2	100.077	99.942	103.495	
Mean 3	116.872	80.688	96.908	
Extreme difference	42.415	30.087	12.492	

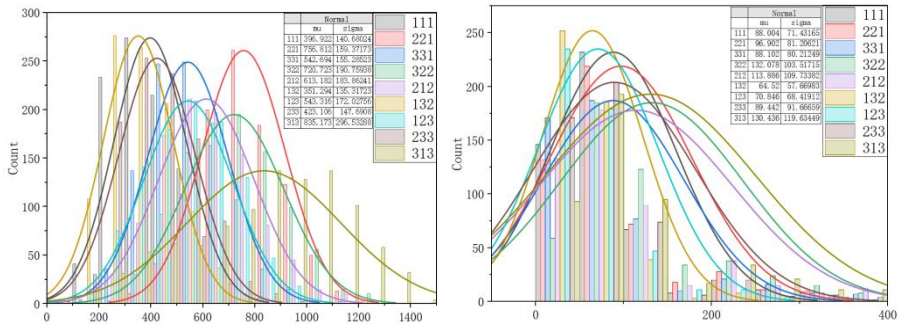

Fig. 6 - Normal Distribution Plot of Wheat and Straw Impact Test

(a) Wheat Impact Test; (b) Straw Impact Test

From the analysis of the orthogonal experiment results for wheat, it can be obtained that, based on the range of the mean values of the influencing factors across different groups, the installation height has the greatest impact on the sensor data, followed by the installation angle, and then the conveyor belt speed. When the installation height was 550 mm, the sensitive plate inclination angle was 40°, and the conveyor belt speed was 8 m/min, the value obtained from wheat impacting the sensitive plate reached its maximum. From the analysis of the orthogonal experiment results for straw, it can be obtained that when the installation height was 350 mm, the sensitive plate inclination angle was 45°, and the conveyor belt speed was 2.7 m/min, the value obtained from straw impacting the sensitive plate reached its minimum.

RESULTS

Response Surface Methodology for Validating Experimental Factors

Based on the orthogonal experimental results, the experiments were analyzed. Quadratic regression fitting analysis was performed on the experimental data using Design-Expert software, and analysis of variance was conducted for wheat and straw, as shown in Tables 5 and 6. The results indicate that the P-values for both the wheat and straw models were less than 0.0001 (significant), while the P-values for the lack of fit were greater than 0.05 (not significant), demonstrating good model fitting. The R^2 values for both the wheat and straw models exceeded 0.99, and the differences between the adjusted and predicted coefficients were less than 0.2, confirming that the models accurately fit the experimental data. The response surfaces illustrating the effects of interactions among the vertical installation height from the conveyor belt plane to the sensitive plate center, the horizontal tilt angle of the sensitive plate, and the conveyor belt speed on the sensor readings are presented in Figure 7.

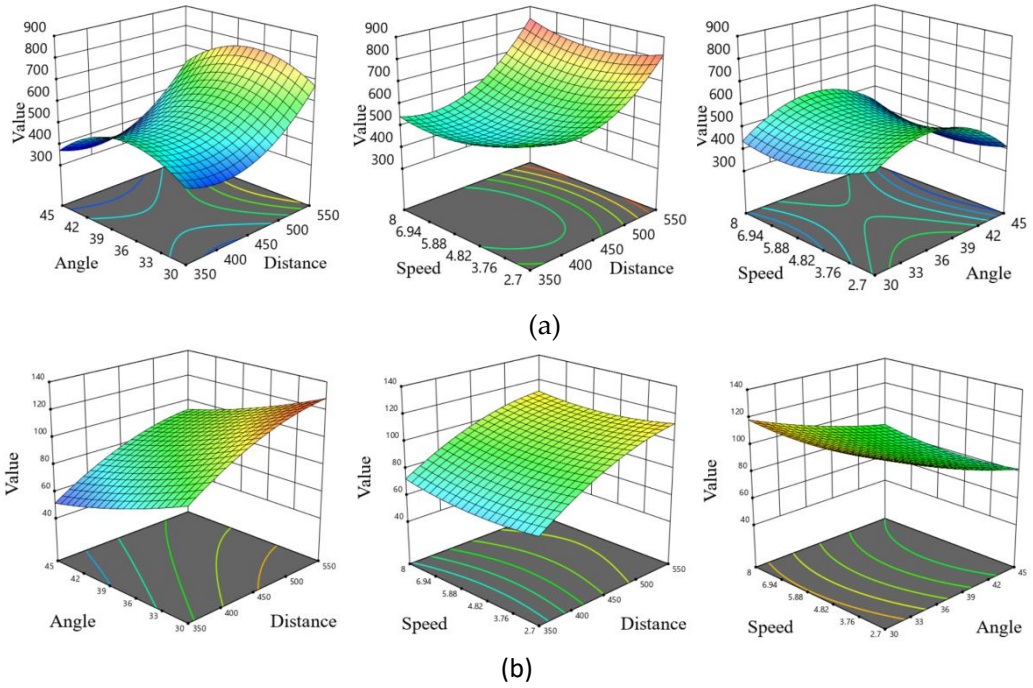

Fig. 7 - Response Surface of Sensor Data for Wheat and Straw Impact on the Sensitive Plate.
(a) Wheat; (b) Straw.

According to the regression model, under the condition of maximizing the target value for wheat, the optimal solution provided by the software was a vertical installation height from the conveyor belt plane to the center of the sensitive plate of 550 mm, a horizontal inclination angle of the sensitive plate of 37.5°, and a conveyor belt speed of 8.0 m/min. Under the condition of minimizing the target value for straw, the optimal solution provided by the software was a vertical installation height of 350 mm, a horizontal inclination angle of 45°, and a conveyor belt speed of 2.7 m/min. It can thus be seen that the optimal conditions corresponding to different materials obtained through response surface analysis were essentially the same as those obtained from the orthogonal experiments. This confirms that these conditions represent the optimal choices for the respective materials.

To better distinguish between wheat and straw, each mean value of wheat under the same influencing factor was subtracted from the corresponding mean value of straw. The condition yielding the maximum difference was selected as the optimal condition for threshold-based discrimination. As shown in Table 7, the optimal choice was an installation height of 550 mm, a sensitive plate inclination angle of 40°, and a conveyor belt speed of 8 m/min. Under these conditions, the discrimination between material ADC values was highest, and the threshold boundary was clearest. Under these conditions, the loss rate calculation achieved the best effect, and the recognition performance was optimal.

Table 5

Analysis of Means

	Factor 1			Factor 2			Factor 3		
	Mean 1	**Mean 2**	**Mean 3**	**Mean 1**	**Mean 2**	**Mean 3**	**Mean 1**	**Mean 2**	**Mean 3**
Wheat	430.534	597.700	699.530	615.116	673.617	439.031	565.499	561.733	600.532
Straw	74.457	100.077	116.872	110.775	99.942	80.688	91.003	103.495	96.908
difference	356.077	497.623	582.658	504.341	573.675	358.343	474.496	458.238	503.624

Determine the threshold for the optimal experimental factors

Wheat grains and wheat straw segments ranging from 50 mm to 150 mm in length were selected as experimental objects, with independent experiments conducted for each material type. For each experiment, 1000 wheat grains and 400 straw segments were randomly selected from the material stock as experimental samples. The experimental conditions were set as follows: the vertical distance from the conveyor belt plane to the sensitive plate was 550 mm, the angle between the sensitive plate and the horizontal plane was 40°, and the conveyor belt speed was 8 m/min. The normal distribution plot of the experimental results is shown in Figure 8.

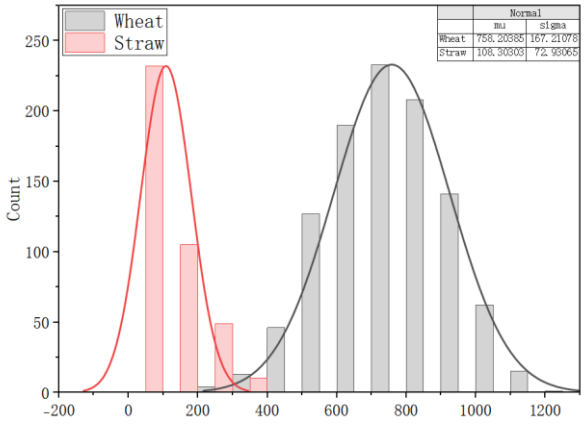

Fig. 8 - Normal Distribution Plot for the Threshold Determination Experiment of Wheat and Straw

Based on the analysis of normal distribution characteristics, the interval where the ADC value of wheat is greater than 423 (i.e., μ-2σ) covers approximately 95.45% of the data, while the interval where the ADC value of straw is less than 254 (i.e., μ+2σ) also covers approximately 95.45% of the data. Accordingly, 423 was set as the lower limit of the determination threshold for wheat, and 254 was set as the upper limit of the determination threshold for straw. For samples with ADC values between 254 and 423, discrimination was performed based on the distribution characteristics of the data within a sliding window.

Experimental Verification and Analysis

To verify the accuracy of the experiment, wheat grains and wheat straw were randomly selected for testing. The experimental conditions were set as follows: the vertical height from the conveyor belt plane to the center of the sensitive plate was 550 mm, the installation angle of the sensitive plate was 40°, and the conveyor belt speed was 8 m/min. The experimental results are shown in Table 6. According to the experimental results, the recognition rate for cleaning loss can reach over 97%.

Table 6

Wheat and Straw Impact Experiments

Types	Manual inspection of actual quantity per unit	Number of sensors detected/per unit	Sensor error	error rate
Wheat	453	448	5	1.1%
Straw	393	382	11	2.8%

CONCLUSIONS

Addressing the practical requirements for detecting cleaning loss rates in wheat combine harvesters, this study designed and developed a cleaning loss detection device based on vibration signal analysis of a sensitive plate. Through a research approach combining theoretical analysis, simulation verification, and bench experiments, the following conclusions were drawn:

(1) A loss detection method utilizing discrete element simulation and signal processing techniques was established. Discrete element models of wheat grains and straw were constructed using Blender and EDEM software. Simulation analysis revealed significant differences in contact force and contact time between the two materials when impacting the sensitive plate, and it was determined that material motion trajectories did not result in secondary contact with the plate. The feasibility of material identification through the detection of impact-generated vibration signals was demonstrated theoretically, providing a theoretical basis for device design.

(2) Through three-factor three-level orthogonal experiments and range analysis, the order of influence of various factors on the impact signal was clarified. The optimal parameter combination for achieving the most significant differentiation between wheat and straw was determined as follows: installation height of 550 mm, sensitive plate inclination angle of 40°, and conveyor belt speed of 8 m/min. Verification experiments confirmed that under these parameters, the difference in the distribution intervals of ADC values for the materials was maximized, laying the foundation for precise threshold setting. Specifically, the ADC values of wheat samples were predominantly distributed in the interval ≥423, while the ADC values of straw were mostly below 254.

(3) Real-time and accurate calculation of the cleaning loss rate was achieved. Through bench experiments, the signal threshold ranges for wheat grains and straw impacting the sensitive plate were calibrated, enabling precise material identification and classification. Experimental results demonstrated that the recognition accuracy of the device for both wheat grains and straw reached 97%, with an overall detection error of less than 3%. This provides important theoretical support and data foundation for the popularization and application of the cleaning loss detection device in practical operational scenarios.

ACKNOWLEDGEMENT

This research was funded by the Special Fund for the China Agriculture Research System, grant number CARS-03.

REFERENCES

[1] Chen, G., Wu, X., Zhang, J., et al. (2025). A flexible cleaning loss sensing module for wheat combine harvesters with reduced error using vertically distributed PVDF sensing array. *Applied Engineering in Agriculture*, Vol. 41, pp. 227-236, United States.

[2] Ding, L., Xu, Y., Qu, Z., Dou, Y., Wang, W., Li, H. (2023). Design of test device for monitoring loss of wheat harvester during cleaning based on EDEM (基于 EDEM 小麦收获机清选损失监测试验装置设计). *Journal of Chinese Agricultural Mechanization*, Vol. 44, pp. 13-21, Jiangsu/China.

[3] Du, Y., Zhang, L., Mao, E., Li, X., Wang, H. (2022). Design and Experiment of Corn Combine Harvester Grain Loss Monitoring Sensor Based on EMD (基于 EMD 的联合收获机籽粒损失监测传感器设计与试验). *Transactions of the Chinese Society for Agricultural Machinery*, Vol. 53, pp. 158-165, Beijing/China.

[4] Guo, H., Han, J., Lyu, Z., Qiu, S., Dong, Y., Guo, L. (2026). Design and test of cleaning loss monitoring device for oil sunflower combine harvester (油葵联合收获机清选损失监测装置设计与试验). *Journal of Jilin University (Engineering and Technology Edition)*, pp. 1-11, Jilin/China.

[5] Hao, J., Jin, D., Gao, Z., Zhao, J., Zhang, K. (2025). Design and experiment of the vibratory soil crushing device for ma yam harvesting machine based on EDEM (基于 EDEM 的麻山药收获机振动碎土装置设计与试验). *Transactions of the Chinese Society of Agricultural Engineering*, Vol. 41, pp. 90-98, Beijing/China.

[6] Hou, Z., Qiu, Y., Chen, Z., Chen, L., Shao, Z. (2020). Numerical Simulation and Experimental Study on Pelleting Motion Law of Agropyron Seeds under Vibration Force Field. *INMATEH - Agricultural Engineering*, Vol. 62, pp. 299-308, Romania.

[7] Li, M., Wang, Y., Xie, S., Liu, F., Chen, X., Li, X., Liu, W. (2024). Simulation analysis and test of the operation performance of shear vibration co-operation subsoiler based on discrete element method (基于离散元法的切振共作深松机作业性能仿真分析及试验). *Transactions of the Chinese Society of Agricultural Engineering*, Vol. 40, pp. 81-90, Beijing/China.

[8] Liu, D., Gong, Y., Zhang, X., Yu, Q., Zhang, X., Chen, X., Wang, Y. (2022). Edem simulation study on the performance of a mechanized ditching device for Codonopsis planting. *Agriculture*, Vol. 12, pp. 1238, Switzerland.

[9] Liu, X., Chen, J., Zhang, X. (2020). Development of STM32－Based Combine Harvester Cleaning Loss Monitoring Device (基于 STM32 的联合收获机清选损失监测装置的研制). *Journal of Agricultural Mechanization Research*, Vol. 42, pp. 200-204, 210, Heilongjiang/China.

[10] Liu, Y., Li, M., Wang, J., Feng, L., Wang, F., He, X. (2023). Design and Test of Entrainment Loss Detection System for Corn Kernel Direct Harvester (玉米籽粒直收机夹带损失检测系统设计与试验). *Transactions of the Chinese Society for Agricultural Machinery*, Vol. 54, pp. 140-149, Beijing/China.

[11] Ma, F., Wang, L., Wang, C., Wang, Q., Lu, C. (2025). Study on Impact Soil Movement Experiments on Wheat Seeds Based on EDEM. *Agriculture*, Vol. 15, pp. 400, Switzerland.

[12] Ma, Y., Wang, Z., Shi, L., Zhao, W., Sun, B., Dai, F., Li, H. (2025). Determination the intrinsic parameters and calibration of contact parameters for wheat seed particles (冬小麦种子颗粒离散元仿真参数标定). *Journal of China Agricultural University*, Vol. 30, pp. 175-184, Beijing/China.

[13] Ni, J., Mao, H., Pang, F., Zhu, Y., Yao, X., Tian, Y. (2015). Design and Experimentation of Piezoelectric Crystal Sensor Array for Grain Cleaning Loss. *International Journal of Distributed Sensor Networks*, Vol. 2015, pp. 754278, United Kingdom.

[14] Peng, J., Shen, H., Ding, W., Chen, W., Peng, B., Li, X., Hu, L., Wang, G. (2025). Research and analysis of conveyor separation mechanism of light and simple sweet potato combine harvester based on EDEM discrete element method. *Computational Particle Mechanics*, Vol. 12, pp. 3421-3438, Germany.

[15] Qu, Z., Lu, Q., Shao, H., Le, J., Wang, X., Zhao, H., Wang, W. (2024). Design and Test of a Grain Cleaning Loss Monitoring Device for Wheat Combine Harvester. *Agriculture*, Vol. 14, pp. 671, Switzerland.

[16] Shen, H., Wang, B., Wang, G., Wang, Y., Bao, G., Hu, L., Hu, Z. (2023). Research and optimization of the hand-over lifting mechanism of a sweet potato combine harvester based on EDEM. *International Journal of Agricultural and Biological Engineering*, Vol. 16, pp. 71–79, Beijing/China.

[17] Sun, Y., Wang, M., Zhang, C. (2021). Experiment calibration of contact parameters between wheat and conveyor belt (小麦与输送机皮带接触参数的试验标定). *Journal of Henan University of Technology (Natural Science Edition)*, Vol. 42, pp. 113-120, Henan/China.

[18] Walkowiak, M., Nehring, A. (2016). Using ChemDuino, Excel, and PowerPoint as Tools for Real-Time Measurement Representation in Class. *Journal of Chemical Education*, Vol. 93, pp. 778-780, United States.

[19] Wang, Z., Che, D., Bai, X., Hu, H. (2018). Improvement and Experiment of Cleaning Loss Rate Monitoring Device for Corn Combine Harvester (玉米联合收获机清选损失监测装置设计与试验). *Transactions of the Chinese Society for Agricultural Machinery*, Vol. 49, pp. 100-108, Beijing/China.

[20] Wang, W., Liu, W., Yuan, L., Qu, Z., He, X., Lyu, Y. (2020). Simulation and Experiment of Single Longitudinal Axial Material Movement and Establishment of Wheat Plants Model (小麦植株建模与单纵轴流物料运动仿真与试验). *Transactions of the Chinese Society for Agricultural Machinery*, Vol. 51, pp. 170-180, Beijing/China.

[21] Wei, D., Wu, C., Jiang, L., Wang, G., Chen, H. (2023). Design and Test of Sensor for Monitoring Corn Cleaning Loss. *Agriculture,* Vol. 13, pp. 663, Switzerland.

[22] Xing, G., Ge, S., Lu, C., Zhao, B., Liu, Y., Zhou, L. (2025). Design and Experiment of VS - 1D CNN-based Clearing Loss Detection System for Corn Kernel Direct Harvester (基于 VS-1D CNN 的玉米籽粒直收机清选损失检测系统设计与试验). *Transactions of the Chinese Society for Agricultural Machinery*, Vol. 56, pp. 206-216, Beijing/China.

[23] Yang, Y., Zhang, M., Jiang, T., Wang, G., Jiang, L. (2025). Design and Test of Real-Time Detection System for Cleaning Loss of Rapeseed Harvester. *Applied Sciences*, Vol. 15, pp. 792, Switzerland.

[24] Zhang, L., Zhai, Y., Chen, J., Zhang, Z., Huang, S. (2022). Optimization design and performance study of a subsoiler underlying the tea garden subsoiling mechanism based on bionics and EDEM. *Soil and Tillage Research,* Vol. 220, pp. 105375, Netherlands.

[25] Zhao, N., Jin, C., Wang, C., Tang, X., Guo, Z. (2023). Research progress on intelligent technology of grain combined harvester cleaning system (谷物联合收获机清选系统智能化技术研究进展). *Journal of Chinese Agricultural Mechanization*, Vol. 44, pp. 163-170, Jiangsu/China.

[26] Zhang, P., Li, F., Wang, F. (2023). Optimization and test of ginger-shaking and harvesting device based on EDEM software. *Computers and Electronics in Agriculture*, Vol. 213, pp. 108257, Netherlands.